R.Pratheeba et al. International Journal of Recent Research Aspects ISSN: 2349-7688, Special Issue: Conscientious Computing Technologies, April 2018, pp. 977-983

A Spectral approach of AIE in pyrene Schiff base derivatives and Interaction with BSA.

R.Pratheeba[1], S.Gurusamy[2], Dr.A.Mathavan[3]

[1,2,3] PG & Research Department of chemistry ,V.O.Chidambaram College, Thoothukudi

Abstract: - The pyrene Schiff base complexes containing amide (R1), urea (R2) and thiourea (R3) derivatives have been successfully synthesized and characterized by using FT-IR, H1- NMR and EI-MS spectrometry. The derivatives are used for aggregation studies by varying the water fraction (0% - 80%).From the UV-visible absorption studies increase the water fraction from 0% - 70%, the absorption peaks basically remained at the same positions. Then further increased water fraction at f_w=80% the absorption peak suddenly decreased. At the same time, levelled – off tails appeared in the visible region in the range of 450 – 600nm. These spectra indicate that the formation of nano aggregate. The receptors in emission studies increase the water fraction 0% to 80% increase the intensity. The emission intensity enhancements due to restricted intermolecular rotation (RIR). The SEM and AFM spectral studies shows that the size of the receptor compounds are in the range from 100-500 nm, which confirms that there is an aggregation of particles in nano size. The interaction between receptor compounds with BSA. The binding studies characterised by UV-vis absorption and fluorescence emission spectral studies. The fluorescence emission spectral studies confirm that the fluorescent intensity of receptors compounds enhances gradually by increasing the concentration of BSA.

Keywords: Restricted Intramolecular Rotation (RIR) and Bovine Serum Albumin (BSA).

1. INTRODUCTION

In recent years, appropriate design and synthesis of efficient, stable, organic fluorescent materials has been a subject of interest in the area of organic light-emitting diodes A (OLEDs)[1,2]. The OLED materials possess a potential for application in next generation flat panel displays and solid-state lighting [3−5].The phenomenon in which organic luminophores show higher photoluminescence efficiency in the aggregated state in solution is called aggregation-induced emission enhancement (AIEE) [6]. Aggregation-caused quenching refers to any process which decreases the fluorescence intensity of a given substance. A variety of processes can result in quenching, such as excited state reactions, energy transfer, complex-formation and collisional quenching [7]. In 2001, Tang and co-workers reported the first AIE active compounds based on the pentaphenyl derivatives of weak fluorescent nature in solution but exhibiting intense fluorescence after aggregation.[8] The fluorescence quantum yields of luminophores in aggregates is found to be a few hundred times higher than those quantum yields in solutions. They also reported that the mechanism of AIE is associated with the restriction of intramolecular rotation (RIR) of chromophoric compound [9]. A number of aggregation-induced emission (AIE) dyes have attracted increasing attention because they show no or weak emission in the solubilised state, but become progressively emissive when forming aggregates. Unlike “conventional” dyes, AIE-active dyes are typically non-planar but show a propeller shape, with a stator moiety surrounded by a number of aryl rotors. In a diluted solution, these rotors are able to freely rotate, thus rendering the dyes non-emissive by dissipating the energy through non-radiative pathways rather than fluorescence emission. In the aggregated state

where the overall propeller shape prevents stacking formation, and thus the dyes become emissive as the excess energy can now be released as light [10].Schiff bases are recognized as having simple synthetic steps and are also applied to many optical sensors [11], as well as in AIE applications. However, to develop Schiff bases with sensor and AIE properties, the presence of strong fuorophores are required [12]. Pyrene and anthracene derivatives were evidenced as excellent fuorophores and widely used in the developments of fuorescence (FL) sensors because of their excellent photoluminescence properties and chemical stabilities. Furthermore, pyrene and anthracene fluorescent probes self-assembled to form dimeric structures upon the addition of certain metal cations to give P–P* and A–A* excimer fluorescence and also provided the AIE characteristics by tuning the solvent conditions as reported previously [13-14].Aggregation-induced enhanced emission (AIEE) probes have been applied to monitor metal ions in many biological and environmental systems [15-19]. The development of AIEE probes for the detection of metal ions has also become an exciting research field [20-21]. The fabrication of such probes with synthetic ease, especially for important ions such as Fe3+, with the required sensitivity and selectivity is an important task that can enrich the toolbox of analytical chemistry in complex systems. This is in addition to the classical analytical methods with sophisticated instruments such as atomic absorption spectroscopy [22–25].

II. Experimental

Materials

1-pyrenecarboxaldehyde, Benzohydrazide, 4-phenylsemicarbazide and 4-phenylthiosemicarbazide were procured from Sigma Aldrich. Then other solvent and chemicals were purchased from commercial sources and used as received.

Instrumentation

The UV-visible absorption spectra were recorded on a JASCO variant 650 spectrophotometer using 1 cm path length cuvette. Emission spectra were measured using a JASCO 630 spectrofluorometer. IR-spectra were recorded on a PerkinElmer Fourier transform infrared (FTIR) spectrometer PARAGON 1000, and 1H nuclear magnetic resonance (NMR) spectra on a Bruker 300 MHz NMR spectrometer. FAB-MS data were obtained using a JEOL, JMS -700 double focusing mass spectrometer. The morphology of the nanoaggregates was studied using scanning electron microscopy (SEM) (Carl Zeiss). The atomic force microscopy (AFM) image was obtained on a Pico Plus AFM instrument (Molecular Imaging Inc., Arizona, USA) operating in the noncontact mode. AFM images were taken under dry conditions. An NCL cantilever was used to scan the sample at a frequency of 177 kHz and a scanning speed2.4 lines/s. Stock solutions for compounds R1–R3 (1 × 10–3 M) were prepared in aqueous THF for BSA binding studies. For binding studies with biomolecules, complexes R1,R2 and R3 were dissolved in 2%THF:98% water (v/v). The sample solution containing BSA (1 mM) was prepared using phosphate buffered saline (PBS) buffer (pH 7.4). The PBS buffer solution was prepared using a mixture of disodium hydrogen phosphate, sodium dihydrogen phosphate and sodium chloride at pH 7.4. Freshly prepared sample solutions were used for each measurement.

General procedure for the preparation of pyrene Schiff based compounds (R1-R3)

The pyrene based receptors (R1-R3) were prepared by reaction of 1-pyrenecarboxaldehyde (0.50 g, 2.17mmol), with corresponding amine (2.39mmol) dissolved in ethanol solution. A few drops of acetic acid were added and refluxed at 75-800C for 3 hours. After the reaction, pyrene derivatives were obtained as golden yellow solids. The reaction mixture was filtered hot, washed with hot ethanol dried under vacuum to obtain a desired product and used without further purification. The yield of the products R1–R3 ranged from 91 to 94%. The prepared compounds were characterized by various spectral techniques.

Characterisation of N'-((1, 8-dihydropyren-1-yl) methylene) benzohydrazide (R1)

Yield: 94%.IR (KBr, cm^{-1}) ν: (C=N) 1550, (N-H) 3214, (C=O) 1643 ;^{1}HNMR (400 MHz, $CDCl_3$): δ 6.99 (s, 1H, J=7.2 Hz, ArH), 7.26 (s, 2H, J=7.2 Hz, ArH), 7.53–7.56 (t, 6H, ArH), 7.59-7.61(d, 2H,J=8.4 Hz, ArH),8.02-8.09 (m, 1H,ArH), 8.13-8.15 (d, 4H, ArH), 8.23-8.24 (d, 4H, ArH), 8.72 (s, 1H, -CH=N) , 9.03 (s, 1H, N-H).ESI-MS (m/z): for $C_{24}H_{18}N_2O$ [M-H+]: calcd. 350.4, found: 347.0; Elemental analysis for $C_{24}H_{18}N_2O$. λ_{max} (nm) Ɛ ($mol.cm^{-1}$) 239 (269737), 288 (215497), 369 (338222).

Characterisation of 1- ((1, 8-dihydropyren-1-yl) methylene) - 4- phenylsemicarbazide (R2)

Yield: 90%. IR (KBr, cm^{-1}) ν: (C=N) 1546, (N-H) 3379, (C=O) 1686;^{1}HNMR (400 MHz, $CDCl_3$): δ 7.10 – 7.15 (t, 1H, J=7.2 Hz, ArH), 7.38 – 7.43(t, 6H, J=7.2 Hz, ArH), 7.78–7.81 (d, 3H, ArH), 8.17 - 8.22(t, 2H,J=8.4 Hz, ArH), 8.32 (s, 1H, ArH), 8.40 - 8.44(m, 6H, ArH), 8.58-8.61 (d, 1H, -CH=N), 9.04-9.06 (d, 1H, -NH), 9.20 (s, 1H, -NH). ESI-MS (m/z): For $C_{24}H_{19}N_3O$ [M-H+]: calcd. 365.4, found: 362.2; Elemental analysis for $C_{24}H_{19}N_3O$. λ_{max} (nm) Ɛ ($mol.cm^{-1}$)238 (143125), 366 (121800), 384 (109525).

Characterisation of 1-((1,8-dihydropyren-1-yl) methylene)- 4-phenylthiosemicarbazide(R3)

Yield: 90%. IR (KBr, cm–1) ν: (C=N) 1594, (N-H) 3287, (C=S) 1489;^{1}HNMR (400 MHz, $CDCl_3$): δ 6.99 (s, 1H, J=7.2 Hz, ArH), 7.26 (s, 1H, J=7.2 Hz, ArH), 7.47 – 7.52(m, 6H, J=7.2 Hz, ArH), 7.52–7.75 (d, 3H, ArH), 8.05 – 8.12(m, 6H,J=8.4 Hz, ArH), 8.17 – 8.23(t, 2H,J=8.4 Hz, ArH), 8.26-

8.30 (t, 4H, ArH), 8.52 - 8.57 (t, 4H, ArH), 8.83-8.86 (d, 1H, ArH), 8.61 (s, 1H, ArH),, 9.04 (s, 1H, -CH=N), 9.27 (s, 1H, -NH), 9.94 (s, 1H, -NH).ESI-MS (m/z): for $C_{24}H_{19}N_3S$ [M-H+]: calcd. 381.5, found: 378.2; Elemental analysis for $C_{24}H_{19}N_3S$. λ_{max} (nm) Ɛ (mol.cm^{-1})238 (189853), 388 (227375), 410 (206262).

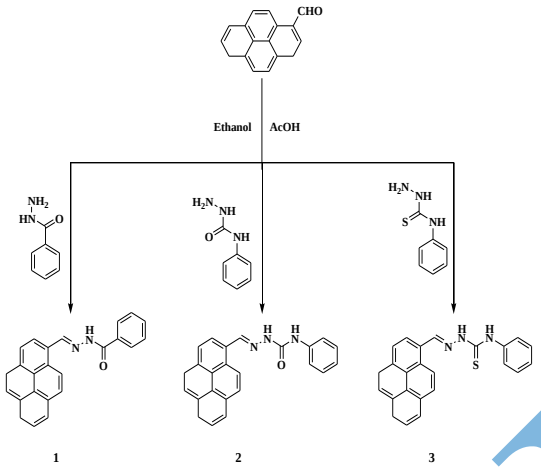

Scheme: 1 Synthetic route for the preparation of pyrene based receptors.

III. Results and Discussion:

Aggregation Induced Emission (AIE) Studies:

UV–visible absorption spectral studies:

The pyrene derivative compounds are involved aggregation in THF-Water (v/v) mixture. The UV–visible absorption spectra of R1–R3 in THF showed an intense band at 236–239 nm with a shoulder at 280–288 nm, corresponding to the π–π* transition of -CZ=C in the aromatic chromophore [26]. The broad band located at 366–388 nm corresponded to n–π* transition of nitrogen atom promoted from their non-bonding molecular orbital to a π anti bonding molecular orbital within the molecule. The absorption spectra of R1–R3 were recorded to check the behaviour of these compounds when different fractions of water were added into the THF solution of these compounds. The UV−visible absorption spectra of R1–R3 (4 μM) in the presence of different percentages of water. Upon addition of water (0–90%), absorbance was decreased in the UV region without any considerable shift in the λ_{max} value [27]. Conversely, on the addition of 90% water, absorbance increased swiftly in the visible region (~500 nm), probably caused by the light scattering or Mie effect of the nanoaggregate suspensions [28]. The results confirmed that R1–R3 underwent aggregation to form nano particles in the aqueous mixture containing 80% of water for both R1 and R2, but 90% of water for R3 and that the solution became slightly turbid. Levelling-off of the tail in the visible region of the absorption spectrum suggested the formation of nanoscopic aggregates of R1–R3.The spectral changes shown in the Figure 1-3.

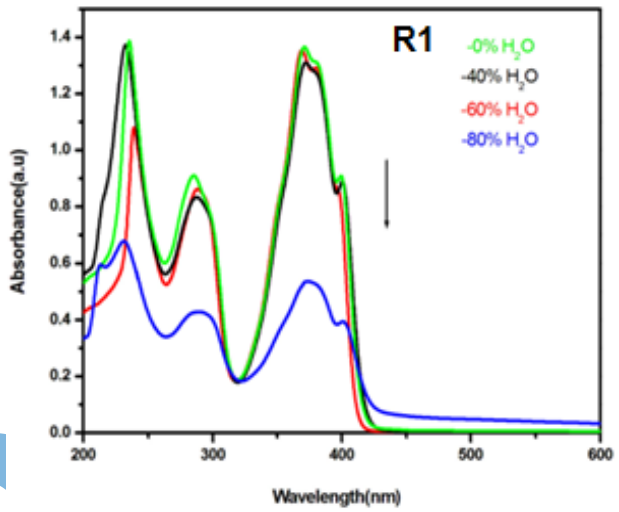

Fig: 1 UV-vis absorption spectra of R1 in THF (4 μM) with increasing percentage of H_2O

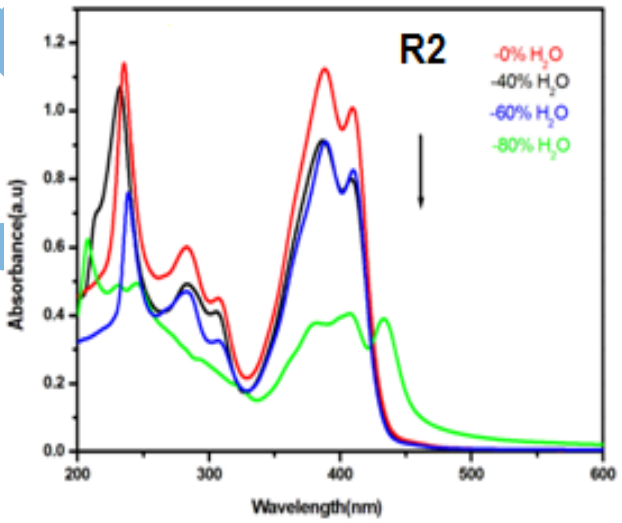

Fig: 2 UV-vis absorption spectra of R2 in THF (4 μM) with increasing percentage of H_2O

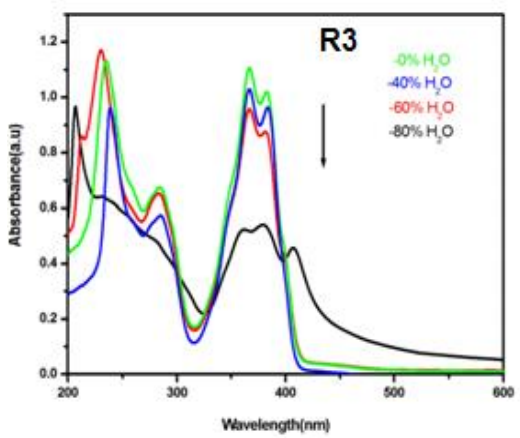

Fig: 3 UV-vis absorption spectra of R3 in THF (4 µM) with increasing percentage of H_2O.

Fluorescence spectral studies:

The emission spectra of these compounds (R1–R3) in THF were recorded; these three compounds exhibited weakly structured emission bands at 450–480 nm upon excitation at 400 nm. Interestingly, upon addition of water to the THF solution of R1 and R2 emission intensity was enhanced more than 10 times with a red shift of about 10 nm from 450 nm to 460 nm. And 439 nm to 449 nm.These spectral changes are shown in the Figure 4-6.indicated that a strong aggregation occurred in the emission spectra at 90% water content. Similar behaviour was also observed with R3emission intensity was enhanced more than 10 times with a red shift of about 11 nm from 429 nm to 440 nm.After the successive addition of water. This emission enhancement was attributed to the restriction of –C=N isomerization of the pyrene rings and thus suppression of the non-radiative pathway and enhancement of fluorescence intensity[29].These compounds were weakly fluorescent due to isomerisation of the C=N bond in the excited state. Fluorescence intensity increased drastically during aggregation due to suppression of C=N isomerization, which deactivated the non-radiative pathway in the excited state [30]. The fluorescence properties of these compounds in solid state thin films have also been investigated. SEM was used to investigate the formation of nanoaggregates and to examine the morphology of aggregates that formed in THF/water mixtures with high f_w (water fraction) values. SEM analysis showed that the R1 aggregate was structurally spherical, whereas R2 had a flower shaped structure, both with a diameter of a few hundred nanometres. When the water fraction was increased from 80% to 90%, the R3 appeared to be clustered nanoparticles. Size decreased, while regularity of morphology increased concomitantly because of the high concentration of water. The difference in morphology indicated that the size and shape of the microstructures correlated with the THF/water ratio and the concentration of the solution. It is believed that in mixtures with a low water fraction the solute molecules steadily assemble in an ordered fashion to form less emissive crystalline aggregates, while in mixtures containing high water content the solute molecules quickly agglomerate in a random way to form highly emissive amorphous particles. The AFM images show that the sizes of compounds R1–R3 were in the range 100–500 nm, confirming the formation of aggregates in the THF/H2Omixture.AFM images of R1–R3 in fw = 80% H2O for R1,R2 and R3 showed that the aggregates were spherical and rod shaped, similar to the SEM images[31]. The images shown in the Fig: 7-8.

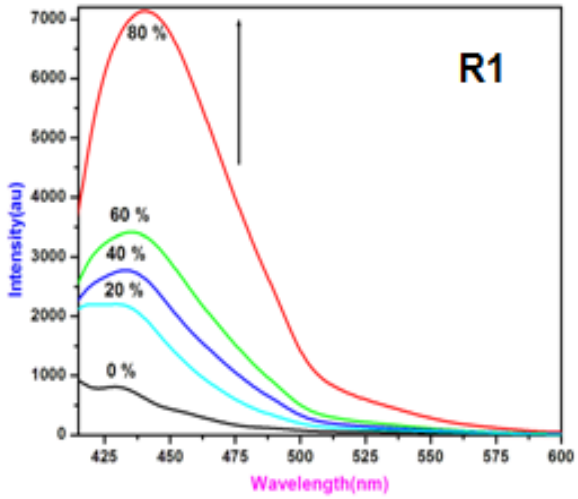

Fig: 4 UV-vis absorption spectra of R1 in THF (4 µM) with increasing percentage of H_2O

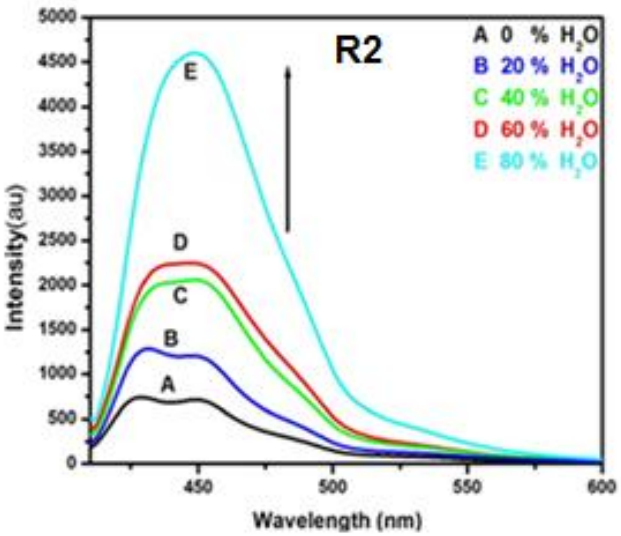

Fig: 5 UV-vis absorption spectra of R2 in THF (4 µM) with increasing percentage of H_2O

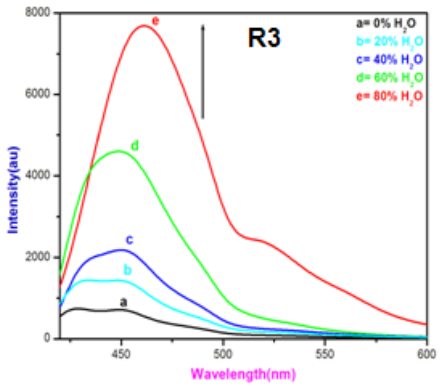

Fig: 6 UV-vis absorption spectra of R3 in THF (4 μM) with increasing percentage of H_2O.

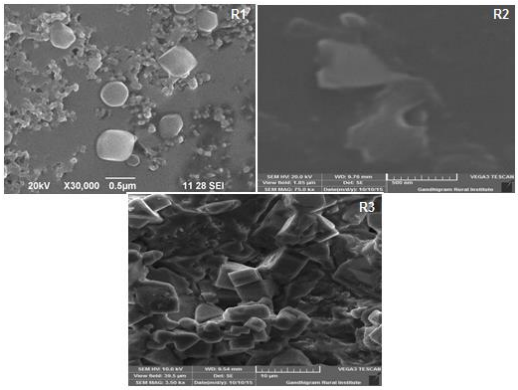

Fig: 7 SEM images of 80 % H_2O of R1-R3.

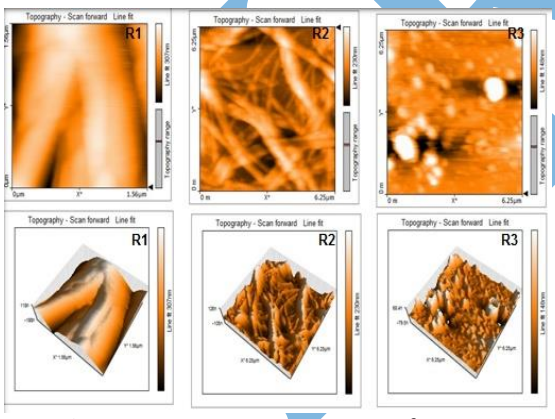

Fig: 8 AFM images 80 % H2O of R1-R3.

Binding studies with BSA:

In order to learn about the binding strength of compounds R1–R3 with BSA, absorption spectral titrations were carried out in aqueous medium. The compound concentration used for the absorption spectral study was fixed at 4 μM and the BSA concentration was varied From 2 μM to 20 μM in phosphate buffer at pH = 7.4.The UV–vis absorption spectra of R1 (4 μM) with gradual addition of BSA. On increasing the BSA concentration, apart from an increase in BSA absorbance at wavelengths 256 and 276 nm, a substantial change in the absorbance intensity of compounds R1–R3 with a slight blue shift was noted. These results showed the strong binding of compounds R1–R3with BSA. These spectral changes clearly implied a change in the probe environment, as the probe was transferred from the aqueous phase to the protein interior [32]. This blue shift observed in the presence of BSA prompted us to propose binding of the protein with these compounds through hydrogen bonding as well as via hydrophobic interactions, and also supported by theoretical studies. The same trend in absorption has been observed in spectral studies shown in the figure: 9. Although BSA showed no absorption at 300–400 nm, addition of BSA led to a substantial increase in absorbance at these wavelengths and these spectral changes were used to calculate the binding constant (K) using equation 1.257 nm in the absence or presence of BSA [33]. εv and εc are the molar extinction coefficients of free and BSA bound compounds, respectively. Therefore, the binding constant (Kb) was estimated from the ratio of the intercept to the slope in the linear double reciprocal plot of 1/(A − A0) versus 1/[BSA]. The binding constant values for the binding of these compounds with BSA calculated from the UV–vis absorption spectral data are given in the Table 1. To confirm the interaction between compounds R1–R3 and proteins, a fluorescence titration was carried out keeping the R1–R3..

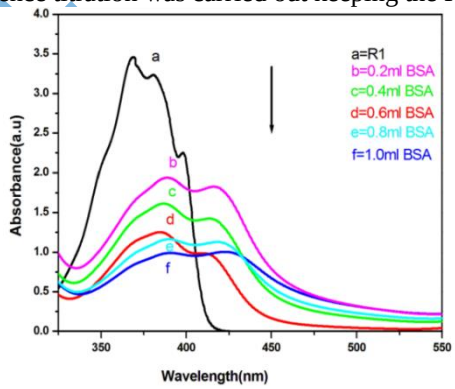

Fig: 9 UV-vis absorption spectra of R1 to R3 in THF (4 μM) with increasing concentrations of BSA.

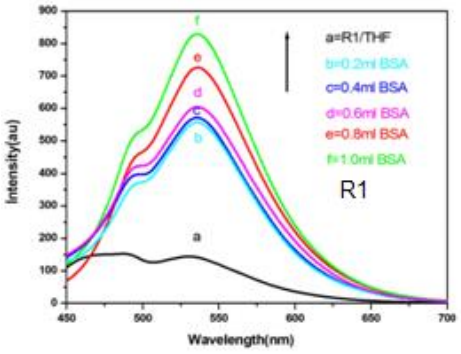

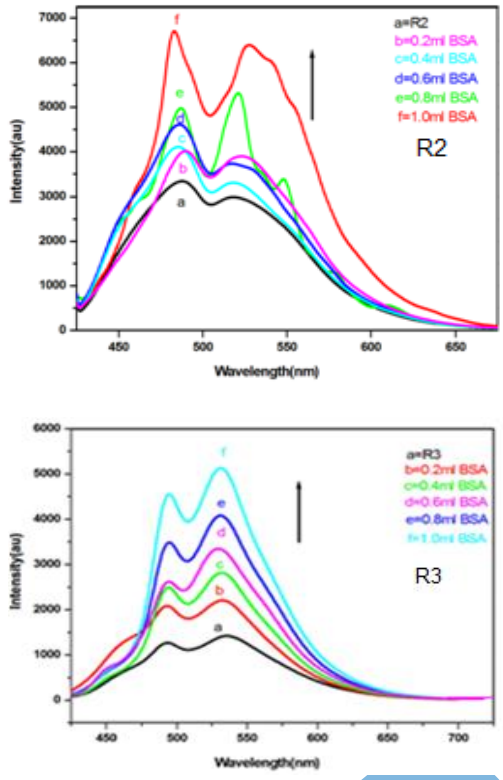

Fig: 10 Emission spectra of R1 to R3 in THF (4 μM) with increasing concentrations of BSA.

The binding constants were calculated using the modified Benesi-Hildebrand equation and are given in the Table: 1

$$\frac{I_0}{I - I_0} = \frac{b}{(a-b)}\left(\frac{1}{K_a[BSA] + 1}\right)$$

Where I and I0 are the luminescence intensities of the Receptors compounds in the presence and absence of BSA, respectively, Ka is the binding constant,a and b are constants. It is interestingly to note that the binding constant values estimated by the absorption as well as the emission spectral study agree well. This may be due to the hydrogen bonding between the Receptors and the BSA.

Receptor	$K_b(M^{-1})$ Absorption	$K_b(M^{-1})$ Emission
R1	$1.5x10^7$	1.7×10^7
R2	1.1×10^7	1.07×10^7
R3	5.6×10^5	5.1×10^5

Table: 1 Binding constants (Kb) values for the interaction of Receptors with BSA

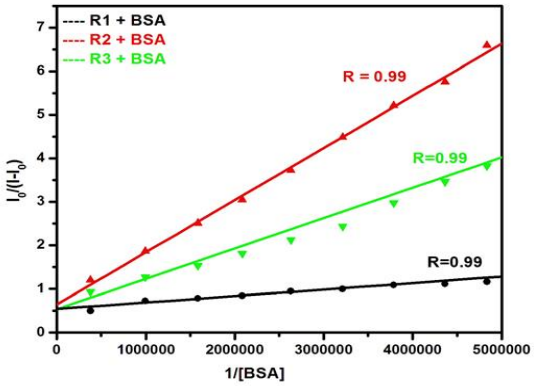

Fig: 11 Plot for the binding of receptor R3 with BSA, [R3] =4μM, [BSA] =10-120μM.

IV. Conclusion

In summary, we have designed three pyrene based receptors comprised of amide, urea and thiourea moieties with AIEE characteristics, which served as excellent fluorescent probes for BSA. In THF, these compounds were weakly emissive but after addition of 90% water the emission intensity was enhanced, due to the AIEE effect and nanoaggregate formation confirmed by microscopic techniques. These compounds bound efficiently with BSA with a binding constant in the order 105–107 M–1 leading to emission enhancement.

References

[1] Chen,C.T. Chem. Mater.2004, 16, 4389−4400.

[2] Yuan, W. Z, Gong, Y. Chen, S. Shen, X. Y. Lam, J. W. Y. Lu, P. Lu, Y.Wang, Z. Hu, R. Xie, N. Chem. Mater. , 2012, 24, 1518−1528.

[3] Reineke,S. Lindner, F. Schwartz, G. Seidler, N. Walzer, K. Lussem, B.; Leo, K. W. Nature., 2009,459, 234−238.

[4] Sun,Y.Giebink, N. C. Kanno, H. Ma, B. Thompson, M. E. Forrest, Nature., 2006, 440, 908−912.

[5] Tonzani, S.. Nature., 2009, 459, 312−314.

[6] Jenekhe,S.A. Osaheni,J.A. Science., 1994, 265, 765−768.

[7] Birks, J. B.Wiley: London, Rietdorf J., Springer, 2005, 246-9.

[8] Luo, J. Xie, Z. Lam, J. W. Y. Cheng, L. Chen, H.Qiu, C. Kwok, H. S. Zhan, X. Liu, Y. Zhu, D. Chem. Commun. 2001, 1740−1741.

[9] Zeng, Q. Li, Z.Dong, Y. Di, C. Qin, A. Hong, Y. Ji, L. Zhu, Z. Jim, C. K. W. Yu, Chem. Commun. 2007, 70 −72.

[10] Hong, Y. Lam, J.W.Y. Tang, B.Z. Chem. Soc. Rev. 2011, 40, 5361–5388.

[11] V. Bhalla, P. Song, X. Chen, Y. Xiang, L. Huang, Z. Zhou, R. Wei and A. Tong, J. Mater. Chem., 2011, 21, 13470.

[12] S. Karupannan and J. C. Chambron,L. Fabbrizzi, M. Lichelli, P. Pallavicini, D. Sacci and E. Taglietti, Chem.–Asian. J, 2011, 6, 964.

[13] M. Kumar, R. Kumar and V. Bhalla, Org. Lett., 2011, 13, 366.

[14] H. J. Kim, S. Bhuniya, R. K. Mahajan, R. Puri, H. Liu, K. C. Ko, J. Y. Lee and J. S. Kim, Chem. Commun., 2009, 7128.

[15] Hong, Y. Lam, J.W.Y. Tang, B.Z.Chem. Soc. Rev. 2011, 40, 5361–5388.

[16] Yuan, Y. Zhang, C.-J. Gao, M. Zhang, R. Tang, B.Z. Liu, B. Chem. Int. Ed. 2015, 54, 1780–1786.

[17] Ding, D. Li, K. Liu, B. Tang, B.Z.Acc. Chem. Res. 2013, 46, 2441–2453.

[18] Liang, J.Tang, B.Z. Liu, B.Chem. Soc. Rev. 2015, 44, 2798–2811.

[19] Hong, Y. Meng, L. Chen, S. Leung,C.W.T.; Da, L.-T.Faisal,M. Silva, D.-A. Liu, J. Lam, J.W.Y.Huang, J. Am. Chem. Soc. 2012, 134, 1680–1689.

[20] Amendola, V.Fabbrizzi, L. Foti, F. Licchelli, M.Mangano, C. Pallavicini, P. Poggi, A. Sacchi, D.Taglietti,A, Coord. Chem. Rev. 2006, 250,273–299.

[21] Yang, Y. Zhao, Q. Feng, W. Li, F.Chem. Rev. 2013, 113,192–270.

[22] Andersen, J.E.T. Analyst .2005, 130, 385–390.

[23] Del Castillo Busto, M.E. Montes-Bayón, M.Blanco -González, E. Meija, J. Sanz-Medel, A. Anal. Chem. 2005, 77, 5615–5621.

[24] Pomazal, K. Prohaska, C. Steffan, I. Reich, G. Huber, J.F. Analyst .1999, 124, 657–663.

[25] Van den Berg, C.M.G. Anal. Chem. 2006, 78, 156–163.

[26] B. Z. Tang, Y. Geng, J. W. Y. Lam, B. Li, X. Jing, X. Wang, F. Wang, A. B. Pakhomov, Chem. Mater. 1999, 11, 1581.

[27] Dong, Y. Q. Lam, J. W. Y. Qin, A. J. Sun, J. X. Liu, J. Z. Li, Z. Sun, J. Z. Sung, H. H. Y. Williams, I. D. Kwok, H. S. Tang, B. Z. Chem. Commun. 2007, 3255–3257.

[28] M.Shellaiah, Yen-Hsing Wu, A. Singh, Mandapati V. R. Raju and H-C Lin. J. Mater. Chem., 2013, 1, 1310.

[29] Y. Hong, J. W. Y. Lam and B. Z. Tang, Chem. Commun., 2009,4332.

[30] Ma, X. F. Cheng, J. H. Liu, J. Y. Zhou, X. G. Xiang, H. F. New J. Chem. 2015, 39 (1), 492−500.

[31] Wang, F. Wen, J. Huang, L. Huang, J. Ouyang, J. Chem.Commun., 2012, 48, 7395−7397.

[32] J. Shobini, A. K. Mishra, K. Sandhya and N. Chandra, Spectrochim. Acta, 2011, 57, 1133–1147.

[33] Ding, L,Z Liu, Y. Cao, Y. Wang, L. Xin, Y. Fang, Y. J. Mater. Chem., 2012, 22, 11574−11582.

